

## Plasma focus ion beam fluence and flux—Scaling with stored energy

S. Lee and S. H. Saw

Citation: [Phys. Plasmas](#) 19, 112703 (2012); doi: 10.1063/1.4766744

View online: <http://dx.doi.org/10.1063/1.4766744>

View Table of Contents: <http://pop.aip.org/resource/1/PHPAEN/v19/i11>

Published by the [American Institute of Physics](#).

---

### Related Articles

Microwave plasma source operating with atmospheric pressure air-water mixtures

[J. Appl. Phys.](#) 112, 093301 (2012)

Observed transition from Richtmyer-Meshkov jet formation through feedout oscillations to Rayleigh-Taylor instability in a laser target

[Phys. Plasmas](#) 19, 102707 (2012)

Alfvén's critical ionization velocity observed in high power impulse magnetron sputtering discharges

[Phys. Plasmas](#) 19, 093505 (2012)

Revisiting plasma hysteresis with an electronically compensated Langmuir probe

[Rev. Sci. Instrum.](#) 83, 093504 (2012)

Coded aperture imaging of fusion source in a plasma focus operated with pure D2 and a D2-Kr gas admixture

[Appl. Phys. Lett.](#) 101, 114104 (2012)

---

### Additional information on [Phys. Plasmas](#)

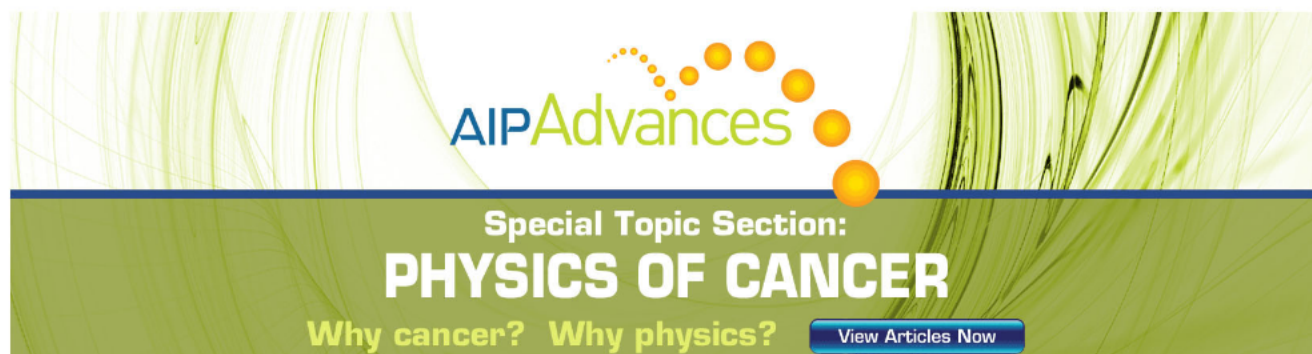
Journal Homepage: <http://pop.aip.org/>

Journal Information: [http://pop.aip.org/about/about\\_the\\_journal](http://pop.aip.org/about/about_the_journal)

Top downloads: [http://pop.aip.org/features/most\\_downloaded](http://pop.aip.org/features/most_downloaded)

Information for Authors: <http://pop.aip.org/authors>

## ADVERTISEMENT



AIPAdvances

Special Topic Section:  
**PHYSICS OF CANCER**

Why cancer? Why physics?

[View Articles Now](#)

# Plasma focus ion beam fluence and flux—Scaling with stored energy

S. Lee<sup>1,2,3,a)</sup> and S. H. Saw<sup>1,2</sup>

<sup>1</sup>INTI International University, 71800 Nilai, Malaysia

<sup>2</sup>Institute for Plasma Focus Studies, 32 Oakpark Drive, Chadstone 3148, Australia

<sup>3</sup>Physics Department, University of Malaya, Kuala Lumpur, Malaysia

(Received 6 September 2012; accepted 24 October 2012; published online 12 November 2012)

Measurements on plasma focus ion beams include various advanced techniques producing a variety of data which has yet to produce benchmark numbers [A Bernard *et al.*, J. Mosc. Phys. Soc. **8**, 93–170 (1998)]. This present paper uses the Lee Model code [S Lee, <http://www.plasmafocus.net> (2012)], integrated with experimental measurements to provide the basis for reference numbers and the scaling of deuteron beams versus stored energy  $E_0$ . The ion number fluence (ions  $\text{m}^{-2}$ ) and energy fluence ( $\text{J m}^{-2}$ ) computed as  $2.4\text{--}7.8 \times 10^{20}$  and  $2.2\text{--}33 \times 10^6$ , respectively, are found to be independent of  $E_0$  from 0.4 to 486 kJ. Typical inductance machines (33–55 nH) produce  $1.2\text{--}2 \times 10^{15}$  ions per kJ carrying 1.3%–4%  $E_0$  at mean ion energy 50–205 keV, dropping to  $0.6 \times 10^{15}$  ions per kJ carrying 0.7%  $E_0$  for the high inductance INTI PF. © 2012 American Institute of Physics. [<http://dx.doi.org/10.1063/1.4766744>]

## I. INTRODUCTION

Measurements of ion beams from plasma focus (PF) devices have produced a wide variety of results using different units, often less correlated than expected, and not giving any discernible pattern or benchmark. In summarizing experimental results<sup>1</sup> in 1996, it was reported that total yields of ions reach  $10^{10}\text{--}10^{14} \text{ sr}^{-1}$  depending on energetics and experimental conditions. In a single discharge, fast ions are emitted from point-like (sub-mm) sources mostly as narrow micro-beams with duration times of 2–8 ns forming intense bunches having total powers reaching  $10^{11}$  to  $10^{12}$  W. Takao *et al.*<sup>2</sup> in 2003, in a 19.4 kJ (43  $\mu\text{F}$ , 30 kV, 500 kA peak current) PF published nitrogen ion beam power brightness of  $0.23 \text{ GW cm}^{-2} \text{ sr}$  (maximum ion energy at 0.5 MeV) using a solid anode and  $1.6 \text{ GW cm}^{-2} \text{ sr}$  (maximum ion energy of 1 MeV) using a hollow anode. Peak ion current densities of  $1100\text{--}1300 \text{ A cm}^{-2}$  (50–60 ns) were recorded. Bhuyan<sup>3</sup> reported beam ion densities of  $9.7\text{--}15.5 \times 10^{19} \text{ m}^{-3}$  (ion energy 15–50 keV) at the aperture of Faraday Cups for  $0^\circ\text{--}25^\circ$  angular positions 6 cm from the anode top in a 40 kV 2.2 kJ neon PF. Track densities (CR-39 film) had a maximum value of  $10.9 \times 10^9$  tracks  $\text{m}^{-2}$  at  $30^\circ$ . Kelly<sup>4</sup> in PF II (4.75 kJ 30 kV) used Faraday Cup and Thomson spectra to measure nitrogen ions (50–1000 keV) recording  $3.2 \times 10^{13}$  ions/sterad with energy content of 0.74 J/sterad. In another experiment,<sup>5</sup> Kelly surmised a total number of  $10^{15}$  deuterons at 20–50 keV from a 10.5  $\mu\text{F}$  30 kV PF. Bhuyan<sup>6</sup> operating a 1.8 kJ methane PF quoted a flux of  $2 \times 10^{22} \text{ m}^{-2} \text{ s}^{-1}$  multiple-charged carbon ions (50–120 keV). Szydlowski<sup>7</sup> using foil-covered CR-39 track detectors states that the PF-1000 generates  $10^5$  ions/ $\text{mm}^2$  (energy above several dozen keV) with neutron yields of  $10^{10}\text{--}10^{11}$  neutrons/shot. Bostick<sup>8</sup> in a 5.4 kJ PF using TOF and ion filters recorded fluence of  $10^{14} (\text{MeV sr})^{-1}$  for the energy spectrum of deu-

terons (0.3–0.5 MeV) with FWHM of 40–60 ns and  $10^{12} (\text{MeV sr})^{-1}$  (at 1–9 MeV) with FWHM of 10–20 ns.

Suffice it to say that the measurement and presentation of results are varied and that it is difficult to assess how these measurements correlate for the purpose of scaling ion beam production across the range of machines. Gribkov *et al.*<sup>9</sup> have taken a more integrated approach. Based on a detailed examination of plasma conditions and energetics within the PF at the time of formation of the plasma diode mechanism,<sup>9</sup> they estimate the following for the PF-1000 operated at 500 kJ: (a) Energy of the electron and ion beam = 20 kJ or 4% of initial stored energy. They comment that these values are conservative when compared to the highest values of 10%–20% reported at Kurchatov, Limeil Laboratory, and Lebedev using different methods. (b) Based on their imaging, assuming cross-section of the ion bunch to be the cross section of the pinch (1 cm radius) and a bunch length of 15 cm giving a bunch volume  $\sim 50 \text{ cm}^3$ , they estimate the total number of ions (average energy 100 keV) in the bunch as  $6 \times 10^{17}$  ions and the concentration of ions within the bunch volume to be  $10^{16} \text{ cm}^{-3}$ . Among published results, Gribkov *et al.* stand out in their presentation which correlates the energetics of the ion beams to the energetics of the system, thus giving a sense of proportion of how the ion beams fit into the overall scheme of things within the PF discharge.

## II. THE METHOD

### A. Defining the fluence and flux of the ion beam

The ion beam exits the PF pinch along its axis. It is a narrow beam (having the same cross-section as the pinch) with little divergence, at least until it overtakes the post-pinch axial shock wave.<sup>9</sup> Hence, the exit beam is best characterized by the ion number per unit cross-section which we term the fluence. We also define the flux as the fluence per unit time of the beam pulse. We compute ion beam number and energy fluence (ions  $\text{m}^{-2}$  and  $\text{J m}^{-2}$ , respectively) and flux (ions  $\text{m}^{-2} \text{ s}^{-1}$  and  $\text{W m}^{-2}$ ) emitted at the upstream end

<sup>a)</sup>Author to whom correspondence should be addressed: Electronic mail: leeing@optusnet.com.au.

of a deuterium PF pinch. We develop an equation for the fluence. We use this equation with the Lee Model code<sup>10</sup> to compute the number and energy fluence and flux and the ion current for any Mather PF. The energy of the fast post-pinch plasma stream is also estimated in the process. The numerical experiments are integrated with each real machine through the computed current trace which is fitted to the measured current trace producing a set of 4 model parameters, the mass swept-up factor  $f_m$  and effective current factor  $f_c$  for the axial phase and  $f_{mr}$  and  $f_{cr}$  for the radial phase.

## B. The Lee model code

The code<sup>10</sup> couples the electrical circuit with PF dynamics, thermodynamics, and radiation. It is energy-, charge- and mass-consistent. It was described in 1983 (Ref. 11) and used in the design and interpretation of experiments.<sup>12–15</sup> An improved 5-phase code incorporating finite small disturbance speed,<sup>16</sup> radiation, and radiation-coupled dynamics was used,<sup>17–19</sup> and was web-published<sup>20</sup> in 2000 and 2005.<sup>21</sup> Plasma self-absorption was included<sup>20</sup> in 2007. It has been used extensively as a complementary facility in several machines, for example, UNU/ICTP PFF,<sup>12,14,15,17–19</sup> NX2,<sup>19,22</sup> NX1,<sup>19</sup> DENA.<sup>23</sup> It has also been used in other machines for design and interpretation including sub-kJ PF machines,<sup>24</sup> FNII,<sup>25</sup> and the UBA hard x-ray source.<sup>26</sup> Information computed includes axial and radial dynamics,<sup>11,17–23</sup> SXR emission characteristics and yield,<sup>17–19,22,27–33</sup> design of machines,<sup>10,12,24,26</sup> optimization of machines,<sup>10,22,24,30</sup> and adaptation to Filippov-type DENA.<sup>23</sup> Speed-enhanced PF<sup>17</sup> was facilitated. Recently, PF neutron yields calculations,<sup>34</sup> current and neutron yield limitations,<sup>35</sup> neutron saturation,<sup>36,37</sup> radiative collapse,<sup>38</sup> current-stepped PF,<sup>39</sup> and extraction of diagnostic data,<sup>33,40–42</sup> and anomalous resistance data<sup>43,44</sup> from current signals have been studied using the code.<sup>10</sup>

## C. The ion beam fluence equation

A detailed description of the model is available on the internet.<sup>10</sup> Neutron yield  $Y_n$  using a phenomenological beam-target neutron generating mechanism<sup>9</sup> was incorporated.<sup>34,35</sup> A beam of fast deuteron ions is produced by diode action in a thin layer close to the anode, with plasma disruptions generating the necessary high voltages. The beam interacts with the hot dense plasma of the focus pinch column to produce the fusion neutrons. The beam-target yield was deduced<sup>34,35</sup> as  $Y_n = Y_{b-t}$

$$Y_{b-t} = C_n n_i I_{\text{pinch}}^2 z_p^2 (\ln(b/r_p)) \sigma / U^{1/2}. \quad (1)$$

Here  $n_i$  = pinch ion density,  $I_{\text{pinch}}$  = current through the pinch;  $r_p$  and  $z_p$  are the final pinch radius and length;  $b$  = cathode radius;  $\sigma$  = cross-section of D-D fusion reaction, n-branch; and  $U$  is the disruption-caused diode voltage.<sup>9</sup> Data fitting gave  $U = 3 V_{\text{max}}$ , where  $V_{\text{max}}$  is the maximum voltage induced by the radially collapsing current sheet; and  $C_n = 8.54 \times 10^8$  (all quantities in SI units) is a constant which was calibrated<sup>34,35</sup> at an experimental point of 0.5

MA from a graphical presentation of all available measured  $Y_n$  data.

The plasma focus  $Y_n$  computed from this model is found to agree well with experiments<sup>10,34–37,45</sup> over all ranges of energy. The agreement is good enough to allow experimental measurements and numerical experimental results to be combined into a global scaling law (neutrons) with a range from sub-kJ to tens of MJ.<sup>37</sup> With the proven success of this model which assumes a deuteron beam interacting with the pinch plasma, we extend the model to extract information about the deuteron beam.

We note that for a beam passing through a plasma target, by definition, cross-section = reaction rate/(beam ion number flux  $\times$  number of target particles). We re-write Eq. (1) using this definition. We obtain

$$Y_{b-t} = (n_b v_b) [n_i (\pi r_p^2 z_p) \tau] \sigma = (J_b \tau) \sigma n_i (\pi r_p^2 z_p). \quad (2)$$

Here  $Y_{b-t}/\tau$  is the D-D fusion reaction rate,  $J_b = n_b v_b$  is the beam ion flux with units of (number of ions  $\text{m}^{-2} \text{s}^{-1}$ ),  $n_b$  = number of beam ions per unit plasma volume traversed,  $v_b$  = beam ion speed; and the number of plasma target particles =  $n_i (\pi r_p^2 z_p)$ ,  $n_i$  being the target plasma ion density; and  $\tau$  = beam-target interaction time assumed to be confinement time of the plasma column. We also denote  $J_b \tau$  as the beam ion fluence with units of (number of ions  $\text{m}^{-2}$ ). This is the ion fluence that is generated by the inductive plasma diode action. From Eqs. (1) and (2), we may write the ion fluence as

$$J_b \tau = C_n I_{\text{pinch}}^2 z_p (\ln(b/r_p)) / (\pi r_p^2 U^{1/2}) \text{ ions } \text{m}^{-2}. \quad (3)$$

As the ion beam traverses the pinch along the axial direction, there is attenuation of the beam due to interaction with the hot dense plasma. However, the proportion of ions that undergoes interactions is small and most of the ions pass through and exit the pinch.<sup>9</sup> We assume that Eq. (3) calculates the number of ions  $\text{m}^{-2}$  exiting the pinch for each PF shot.

## III. THE RESULTS AND DISCUSSIONS

### A. A large machine and a small machine have the same fluence

To illustrate our method, as an example, we run the code for PF1000 (one of the largest PF machines), using typical PF1000 configuration<sup>9,10,34,35,45</sup> at 486 kJ:  $L_0 = 33$  nH,  $C_0 = 1332$   $\mu\text{F}$ ,  $b = 16$  cm,  $a = 11.55$  cm,  $z_0 = 60$  cm  $r_0 = 6.3$  m $\Omega$ , operated at  $V_0 = 27$  kV,  $P_0 = 3.5$  Torr deuterium. Fitted mass and current factors<sup>13,46</sup> are  $f_m = 0.14$ ,  $f_c = 0.7$ ,  $f_{mr} = 0.35$ , and  $f_{cr} = 0.7$ .

Relevant results computed from the code (RADPFV5.15dd)<sup>10</sup> are recorded from the data-line of the active sheet on completion of the numerical shot:  $I_{\text{pinch}} = 862$  kA,  $z_p = 18.8$  cm,  $b/r_p = 16$  cm/2.23 cm,  $U = 3V_{\text{max}} = 3 \times 42$  kV = 126 kV,  $\tau = 245$  ns.

Substituting into Eq. (3), we have the ion fluence:  $J_b \tau = 3.9 \times 10^{20}$  ions  $\text{m}^{-2}$  per shot. Taking  $r_p = 2.23$  cm as the radius of the beam, then number of ions in the

beam =  $6.1 \times 10^{17}$  ions per shot; with mean energy of 126 keV.

For comparison, we run the INTI PF which is one of the machines of the 3 kJ UNU/ICTP PFF<sup>10,12–14,30,33,41–43</sup> network. The configuration is  $L_0 = 110$  nH,  $C_0 = 30$   $\mu$ F,  $b = 3.2$  cm,  $a = 0.95$  cm,  $z_0 = 16$  cm  $r_0 = 12$  m $\Omega$ ; operated at  $V_0 = 15$  kV,  $P_0 = 3.5$  Torr deuterium. The fitted model parameters are  $f_m = 0.073$ ,  $f_c = 0.7$ ,  $f_{mr} = 0.16$ ,  $f_{cr} = 0.7$ .

Relevant data are recorded after the numerical shot:  $I_{\text{pinch}} = 122$  kA,  $z_p = 1.4$  cm,  $b/r_p = 3.2$  cm/0.13 cm,  $U = 3V_{\text{max}} = 3 \times 25$  kV = 75 kV,  $\tau = 7.6$  ns. Thus, the ion fluence  $J_b \tau = 3.6 \times 10^{20}$  ions  $\text{m}^{-2}$ . Number of ions =  $1.9 \times 10^{15}$  per shot; mean energy of 76 keV.

These results indicate that the ion fluence for the 500 kJ PF1000 PF at  $3.9 \times 10^{20}$  ions  $\text{m}^{-2}$  is practically the same as the 3 kJ INTI small PF with  $3.6 \times 10^{20}$  ions  $\text{m}^{-2}$ . The energy fluence of the ion beam is also not correlated to the 140 times difference in  $E_0$ ; the value for the PF1000 being not quite twice higher than for the INTI PF and only due to the higher mean energy of its beam ions.

The number of beam ions for PF1000 is  $6.1 \times 10^{17}$  ions per shot, some 320 times that of the smaller machine. The energy carried in the ion beam for PF1000 is 12 kJ (2.5% of  $E_0$ ), whilst that for the smaller machine is 23 J (0.7%  $E_0$ ). As will be discussed and shown in Table II, the relative inefficiency of the INTI PF is due to its high static inductance  $L_0$ .

## B. Results for a range of machines from 0.4 to 500 kJ

We carried out a series of numerical experiments on a range of machines to obtain the trends across the range of PF. Each machine has its computed current waveform fitted with a measured current waveform so that the computed dynamics and plasma pinch conditions are realistically portrayed. The results are shown in Table I.

From Table I, we note (1) the  $I_{\text{peak}}$  and  $I_{\text{pinch}}$  decrease as  $E_0$  is reduced. This is generally true except for the case of Poseidon and NX2 which exhibit higher performance in  $I_{\text{peak}}$  and  $I_{\text{pinch}}$  due to exceptionally low inductance  $L_0$ . On the other hand, the value of  $I_{\text{peak}}$  and  $I_{\text{pinch}}$  for the 3 kJ INTI PF is particularly low due to its unusually large  $L_0$ . (2) Anode radius “a” correlates<sup>14,28</sup> with  $I_{\text{peak}}$  and  $I_{\text{pinch}}$ . The ratio  $I_{\text{peak}}/a$  is within a small range of 160–240 kA/cm except for the Poseidon which has 486 kA/cm, being designed for unusually high speed operation.<sup>47</sup> Pinch length and pinch radius correlate with “a”.<sup>14,28</sup> (3) The beam duration  $\tau$  varies with “a” from 5 to 255 ns; the ratio  $\tau/a$  has a range of 8–22 ns/cm.<sup>14,28</sup> (4) The beam ion mean energy ranges over 54–292 keV. (5) The ion fluence is  $2.4$ – $7.8 \times 10^{20}$  ions  $\text{m}^{-2}$ , has no correlation with  $E_0$ , and has only small variation through the whole range of  $E_0$ . (6) Due to the dependence of  $\tau$  with “a”, the ion flux has a relatively bigger range of  $1.5$ – $50.4 \times 10^{27}$  ions  $\text{m}^{-2} \text{s}^{-1}$  being greater for the smaller machines. (7) The energy fluence has a variation  $2.2$ – $33 \times 10^6$  J  $\text{m}^{-2}$ . (8) The energy flux varies over the range  $3.1$ – $56.4 \times 10^{13}$  W  $\text{m}^{-2}$ . (9) The number of ions in the beam increases with  $E_0$  being  $6 \times 10^{14}$  for the 0.4 kJ PF-400 J and 1000 times that for the PF1000. (10) The energy of

the beam at pinch exit varies from 0.7% to 5.4%  $E_0$ . (11) The ion beam current ranges from 18.6 to 629 kA being 14%–22% of  $I_{\text{peak}}$ . (12) For applications to materials, a damage factor (Dam fr in Table I) has been defined as energy flux  $\times$  (pulse duration)<sup>0.5</sup> with units of  $\text{Wm}^{-2} \text{s}^{0.5}$ . We find this factor is  $1.6$ – $11 \times 10^{10} \text{Wm}^{-2} \text{s}^{0.5}$  across the whole range of machines. (13) Fast post-pinch plasma stream (PS) energy at pinch exit is estimated to range between 1.3% and 14% of  $E_0$  with streaming speeds ranging 18–49 cm/ $\mu$ s.

We note that our computed values for PF1000 of  $6.1 \times 10^{17}$  ions (mean energy 126 keV) carrying 12.2 kJ of energy compare well with the values of  $6 \times 10^{17}$  ions (mean ion energy 100 keV) carrying 10 kJ of energy estimated by Gribkov *et al.*<sup>9</sup>

Our computed values for ion number and average ion energy are, respectively,  $1.9 \times 10^{15}$  (mean ion energy 75 keV) for the 3.4 kJ INTI PF, comparable with Kelly *et al.*’s measured value of  $10^{15}$  ions at 20–50 keV from their 4 kJ focus.

## IV. CONCLUSIONS-ION BEAM PROPERTIES AND SCALING

The results are summarized in Table II, which gives the range of the deuteron beam properties and the scaling suggested by an inspection of Table I. As a notable example, Table II states that the ion number fluence is  $2.4$ – $7.8 \times 10^{20}$  ions  $\text{m}^{-2}$  varying by a factor 3 through the whole range of  $E_0$  from 0.4 to 486 kJ and independent of  $E_0$  as can be seen by studying the numbers in Table I. Table II suggests that the range of  $2$ – $8 \times 10^{20}$  ions  $\text{m}^{-2}$  may be set as a benchmark for the ion beam number fluence of any Mather PF. The independence of  $E_0$  of the ion beam fluence is likely related to the constancy of energy density (energy per unit mass) that is one of the key scaling parameters of the PF throughout its  $E_0$  range of sub kJ to MJ.<sup>14,28</sup>

The number of beam ions exiting the pinch is found to range from  $6 \times 10^{17}$  ions for the 486 kJ PF1000 to  $6 \times 10^{14}$  for the 0.4 kJ PF-400 J with a strong correlation to  $E_0$ , modified by a dependence on  $I_{\text{peak}}$  (or  $L_0$ ). Table II suggests a benchmark of  $12$ – $20 \times 10^{14}$  beam ions per kJ for PF’s with typical static inductances  $L_0$  of 30–55 nH, dropping to  $6 \times 10^{14}$  beam ions per kJ for the high  $L_0$  INTI PF (indicated by \* in Table II). Correspondingly the high  $L_0$  INTI PF has significantly lower beam energy (<sup>+</sup> in Table II) and beam charge (<sup>#</sup> in Table II).

The ion current may be set as 14%–23% of  $I_{\text{peak}}$ , taking the ion beam pulse duration to be equal to the computed pinch duration which is an approximation that needs to be improved upon. If the beam duration is measured to be higher than the computed pinch duration as seems to be the case for the smaller machines, the ion currents will drop correspondingly. We are in the process of working out how to improve the estimation of ion beam pulse duration.

The range of machines considered in this exercise is wide not just in terms of range of stored energies but also in terms of some stand-out characteristics. For example, the Texas A & M machine, NX3, NX2, PF-5 M, and PF-400 J may be considered to be the more typical plasma focus

TABLE I. A range of plasma focus and computed deuteron beam characteristics.

Machine	PF1000 (Refs. 3, 9, and 10)	Poseidon (Refs. 10 and 47)	Texas (Ref. 48)	DPF78 (Refs. 10 and 49)	NX3 (Ref. 50)	INTI (Refs. 10 and 30)	NX2 (Refs. 10 and 19)	PF5M (Ref. 51)	PF400J (Refs. 10 and 24)
$E_0$ (kJ)	486	281	126	31.0	14.5	3.4	2.7	2.0	0.4
$L_0$ (nH)	33	18	40	55	50	110	20	33	40
$V_0$ (kV)	27	60	30	60	17	15	14	16	28
“a” (cm)	11.50	6.60	5.10	4.00	2.60	0.95	1.90	1.50	0.60
$c = b/a$	1.4	1.5	1.7	1.3	2	3.4	2.2	1.7	2.7
$I_{\text{peak}}$ (kA)	1846	3205	1509	961	582	180	382	258	129
$I_{\text{pinch}}$ (kA)	862	1000	742	444	348	122	220	165	84
$z_p$ (cm)	18.8	11.0	7.7	5.5	3.8	1.4	2.8	2.3	0.8
$r_p$ (cm)	2.23	1.22	0.84	0.62	0.40	0.13	0.31	0.22	0.09
$\tau$ (ns)	254.9	83.0	77.5	41.0	36.5	7.6	30.0	12.2	5.1
$V_{\text{max}}$ (kV)	42	97	67	68.3	35	25	22	32.3	18
Ion fluence ( $\times 10^{20} \text{ m}^{-2}$ )	3.9	7.0	7.8	3.2	5.7	3.6	3.4	2.4	2.6
Ion flux ( $\times 10^{27} \text{ m}^{-2} \text{ s}^{-1}$ )	1.5	8.4	10.0	7.8	15.6	46.7	11.5	19.6	50.4
Mean ion energy (keV)	126	292	201	205	105	75	65	97	54
En fluence ( $\times 10^6 \text{ J m}^{-2}$ )	7.8	33.0	25	10.6	9.6	4.3	3.6	3.7	2.2
En flux ( $\times 10^{13} \text{ W m}^{-2}$ )	3.1	39.0	32	25.8	26.3	56.4	12.0	30.6	43.2
Ion number ( $\times 10^{14}$ )	6100	3300	1700	390	280	19	110	37	5.9
FIB energy (J)	12248	15270	5540	1284	479	23	111	58	5
FIB energy ( $\%E_0$ )	2.5	5.4	4.4	4.1	3.3	0.7	4.1	2.1	1.3
IB current (kA)	380.0	629.0	355	152.4	124.8	40.0	56.7	49.1	18.6
Dam Fr ( $\times 10^{10} \text{ W m}^{-2} \text{ s}^{0.5}$ )	1.6	11.0	9.0	5.2	5.0	4.9	2.1	3.4	3.1
Ion speed (cm/ $\mu\text{s}$ )	347	528	438	443	317	269	250	305	226
Ion number/kJ ( $\times 10^{14}$ )	12.6	11.7	13.5	12.7	19.4	5.6	40.1	18.1	15.1
Plasma stream En (J)	39120	30152	11700	394	1707	249	369	92	17
P S En ( $\%E_0$ )	8.1	10.7	9.3	1.3	12.0	7.4	14.0	4.5	4.5
PS speed (cm/ $\mu\text{s}$ )	18.2	37.2	23.2	23.1	24.2	47.4	20.1	48.6	35.7

devices with static inductance  $L_0$  in a good performance range of 20–50 nH, operating voltage between 14 and 30 kV, and the capacitor banks being lightly damped. The DPF78 is also within this range of “typical” machines except that it operates at a higher voltage of 60 kV. These 6 machines operate with similar speed factors<sup>14</sup> indicative of end axial speeds close to 10 cm/ $\mu\text{s}$ . The INTI PF is one of the network of UNU/ICTP PFF machines having conventional single-capacitor configuration, hence a rather large  $L_0$  of 110 nH. Such large  $L_0$  machines (Type 2) have

a significantly different pre- and post-focus energy distribution characteristics compared with the more “typical” higher performance (Type 1)  $L_0$  range of 20–50 nH.<sup>43</sup> The PF1000 is also within the “typical” range of machines in the aspects (static inductance, speed factor, and operational voltage) mentioned above, but it is not typical in that its capacitor bank is much more heavily damped which has an effect on its performance.<sup>34,35</sup> The Poseidon is atypical in the important aspect of a very high speed factor, more than twice that of all the other machines. It is also unusually high in operating voltage and outstandingly low in static inductance. Including this specially “high”-performance machine Poseidon on the one hand, and the specially high  $L_0$  machine the INTI PF on the other extreme in Table I, it is notable that the variation of fluence and of ion number per kJ may be considered as remarkably small in view of the extreme “atypical” characteristics of these two machines within the range of machines considered as discussed above. In a future exercise, a matrix will be designed to consider a range of machines with more uniform characteristics in order to obtain data with less variation so as to present more definite scaling rules. Other gases will also be considered.

With this method, ion beam and fast plasma stream parameters may be computed for any Mather-type plasma focus. These numerical experiments will place ion beam diagnostics on a firmer footing, complement and guide experiments, and provide a firmer basis for estimating expected effects on target materials.

TABLE II. Summary of range of ion beam properties and suggested scaling.

Property	Units (multiplier)	Range	Suggested scaling
Fluence	Ions $\text{m}^{-2}$ ( $\times 10^{20}$ )	2.4–7.8	Independent of $E_0$
Average ion energy	keV	54–292	Independent of $E_0$
Energy fluence	$\text{J m}^{-2}$ ( $\times 10^6$ )	2–33	Independent of $E_0$
Beam exit radius	fraction of radius “a”	0.14–0.19	Scales with “a”
Beam ion number	Ions per kJ ( $\times 10^{14}$ )	12–40*	Scales with $E_0$
Beam energy	$\%$ of $E_0$	1.3–5.4 <sup>+</sup>	Scales with $E_0$
Beam charge	mC per kJ	0.2–0.6 <sup>#</sup>	Scales with $E_0$
Beam duration	ns per cm of “a”	8–22	Scales with “a”
Flux	ions $\text{m}^{-2} \text{ s}^{-1}$ ( $\times 10^{27}$ )	1.5–50	Independent of $E_0$
Energy flux	$\text{W m}^{-2}$ ( $\times 10^{13}$ )	3–56	Independent of $E_0$
Beam current	$\%$ of $I_{\text{peak}}$	14–23	Scales with $I_{\text{peak}}$
Damage factor	( $\times 10^{10} \text{ W m}^{-2} \text{ s}^{0.5}$ )	1.6–11	Independent of $E_0$

\* = 6 for INTI PF  
<sup>+</sup> = 0.7 for INTI PF  
<sup>#</sup> = 0.1 for INTI PF

## ACKNOWLEDGMENTS

This work was carried out within the framework of IAEA Research Contract No. 16934 of CRP F1.30.13 (Investigations of Materials under High Repetition and Intense Fusion-relevant Pulses). The authors acknowledge a discussion with Paul C. K. Lee which led to the initiation of this project.

- <sup>1</sup>A. Bernard, H. Bruzzone, P. Choi, H. Chuaqui, V. Gribkov, J. Herrera, K. Hirano, A. Krejci, S. Lee, C. Luo, F. Mezzetti, M. Sadowski, H. Schmidt, K. Ware, C. S. Wong, and V. Zoita, *J. Mosc. Phys. Soc.* **8**, 93–170 (1998).
- <sup>2</sup>K. Takao, T. Honda, I. Kitamura, and K. Masugata, *Plasma Sources Sci. Technol.* **12**, 407–411 (2003).
- <sup>3</sup>M. Bhuyan, N. K. Neog, S. R. Mohanty, C. V. S. Rao, and P. M. Raole, *Phys. Plasmas* **18**, 033101 (2011).
- <sup>4</sup>H. Kelly, A. Lepone, A. Márquez, M. Sadowski, J. Baranowski, and E. Skladnik-Sadowska, *IEEE Trans. Plasma Sci.* **26**, 113 (1998).
- <sup>5</sup>P. H. Kelly and A. Márquez, *Plasma Phys. Controlled Fusion* **38**, 1931–1942 (1996).
- <sup>6</sup>H. Bhuyan, H. Chuaqui, M. Favre, I. Mitchell, and E. Wyndham, *J. Phys. D: Appl. Phys.* **38**, 1164–1169 (2005).
- <sup>7</sup>A. Szydłowski, A. Banaszak, B. Bienkowska, I. M. Ivanova-Stanik, M. Scholz, and M. J. Sadowski, *Vacuum* **76**, 357–360 (2004).
- <sup>8</sup>W. H. Bostick, H. Kilic, V. Nardi, and C. W. Powell, *Nucl. Fusion* **33**, 413–420 (1993).
- <sup>9</sup>V. A. Gribkov, A. Banaszak, B. Bienkowska, A. V. Dubrovsky, I. Ivanova-Stanik, L. Jakubowski, L. Karpinski, R. A. Miklaszewski, M. Paduch, M. J. Sadowski, M. Scholz, A. Szydłowski, and K. Tomaszewski, *J. Phys. D: Appl. Phys.* **40**, 3592–3607 (2007).
- <sup>10</sup>S. Lee, Radiative Dense Plasma Focus Computation Package: RADPF, <http://www.plasmafocus.net>; <http://www.intimal.edu.my/school/fas/UFLF/> (archival websites) (2012).
- <sup>11</sup>S. Lee, in *Radiation in Plasmas*, edited by B. McNamara, Proceedings of Spring College in Plasma Physics, ICTP, Trieste, 1983 (World Scientific, Singapore, 1984), Vol. II, pp. 978–987.
- <sup>12</sup>S. Lee, T. Y. Tou, S. P. Moo, M. A. Elissa, A. V. Gholap, K. H. Kwek, S. Mulyodrono, A. J. Smith, Suryadi, W. Usala and M. Zakaulah, *Am. J. Phys.* **56**, 62 (1988).
- <sup>13</sup>T. Y. Tou, S. Lee, and K. H. Kwek, *IEEE Trans. Plasma Sci.* **17**, 311–315 (1989).
- <sup>14</sup>S. Lee and A. Serban, *IEEE Trans. Plasma Sci.* **24**, 1101–1105 (1996).
- <sup>15</sup>S. P. Moo, C. K. Chakrabarty, and S. Lee, *IEEE Trans. Plasma Sci.* **19**, 515–519 (1991).
- <sup>16</sup>D. E. Potter, *Phys. Fluids* **14**, 1911 (1971).
- <sup>17</sup>A. Serban and S. Lee, *Plasma Sources Sci. Technol.* **6**, 78 (1997).
- <sup>18</sup>M. H. Liu, X. P. Feng, S. V. Springham, and S. Lee, *IEEE Trans. Plasma Sci.* **26**, 135 (1998).
- <sup>19</sup>S. Lee, P. Lee, G. Zhang, X. Feng, V. A. Gribkov, M. Liu, A. Serban, and T. Wong, *IEEE Trans. Plasma Sci.* **26**, 1119 (1998).
- <sup>20</sup>S. Lee, <http://ckplee.home.nie.edu.sg/plasmaphysics/> (archival website), 2012.
- <sup>21</sup>S. Lee, ICTP Open Access Archive, <http://eprints.ictp.it/85/>, 2005.
- <sup>22</sup>D. Wong, P. Lee, T. Zhang, A. Patran, T. L. Tan, R. S. Rawat, and S. Lee, *Plasma Sources Sci. Technol.* **16**, 116 (2007).
- <sup>23</sup>V. Siahpoush, M. A. Tafreshi, S. Sobhanian, and S. Khorram, *Plasma Phys. Controlled Fusion* **47**, 1065 (2005).
- <sup>24</sup>L. Soto, P. Silva, J. Moreno, G. Silvester, M. Zambra, C. Pavez, L. Altamirano, H. Bruzzone, M. Barbaglia, Y. Sidelnikov, and W. Kies, *Braz. J. Phys.* **34**, 1814 (2004).
- <sup>25</sup>H. Acuna, F. Castillo, J. Herrera, and A. Postal, in International conference on Plasma Science, 3–5 June 1996, conf record Pg127.
- <sup>26</sup>C. Moreno, V. Raspa, L. Sigaut, R. Vieytes, and A. Clausse, *Appl. Phys. Lett.* **89**, 91502 (2006).
- <sup>27</sup>S. Lee, R. S. Rawat, P. Lee, and S. H. Saw, *J. Appl. Phys.* **106**, 023309 (2009).
- <sup>28</sup>S. H. Saw and S. Lee, *Energy Power Eng.* **2**(1), 65–72 (2010).
- <sup>29</sup>M. Akel, Sh. Al-Hawat, S. H. Saw, and S. Lee, *J. Fusion Energy* **29**(3), 223–231 (2010).
- <sup>30</sup>S. H. Saw, P. C. K. Lee, R. S. Rawat, and S. Lee, *IEEE Trans. Plasma Sci.* **37**, 1276–1282 (2009).
- <sup>31</sup>M. Akel, S. Lee, and S. H. Saw, Numerical Experiments in Plasma Focus Operated in Various Gases, *IEEE Trans Plasma Sci* (accepted for publication).
- <sup>32</sup>M. Akel, S. Lee, and S. H. Saw, “Numerical experiments in plasma focus operated in various gases,” *IEEE Trans. Plasma Sci.* (accepted for publication).
- <sup>33</sup>S. Lee, S. H. Saw, R. S. Rawat, P. Lee, A. Talebitahter, A. E. Abdou, P. L. Chong, F. Roy, A. Singh, D. Wong, and K. Devi, *IEEE Trans. Plasma Sci.* **39**, 3196–3202 (2011).
- <sup>34</sup>S. Lee and S. H. Saw, *J. Fusion Energy* **27**, 292–295 (2008).
- <sup>35</sup>S. Lee and S. H. Saw, *Appl. Phys. Lett.* **92**, 021503 (2008).
- <sup>36</sup>S. Lee, *Plasma Phys. Controlled Fusion* **50**, 105005 (2008).
- <sup>37</sup>S. Lee, *Appl. Phys. Lett.* **95**, 151503 (2009).
- <sup>38</sup>S. Lee, S. H. Saw, and J. Ali, *J. Fusion Energy* **31**, 603 (2012).
- <sup>39</sup>S. Lee, S. H. Saw, and J. Ali, *J. Fusion Energy* (published online).
- <sup>40</sup>S. Lee, S. H. Saw, P. C. K. Lee, R. S. Rawat, and H. Schmidt, *Appl. Phys. Lett.* **92**, 111501 (2008).
- <sup>41</sup>S. H. Saw, S. Lee, F. Roy, P. L. Chong, V. Vengadeswaran, A. S. M. Sidik, Y. W. Leong, and A. Singh, *Rev. Sci. Instrum.* **81**, 053505 (2010).
- <sup>42</sup>S. Lee, S. H. Saw, R. S. Rawat, P. Lee, R. Verma, A. Talebitahter, S. M. Hassan, A. E. Abdou, M. Ismail, A. Mohamed, H. Torreblanca, Sh. Al. Hawat, M. Akel, P. L. Chong, F. Roy, A. Singh, D. Wong, and K. Devi, *J. Fusion Energy* **31**, 198–204 (2012).
- <sup>43</sup>S. Lee, S. H. Saw, A. E. Abdou, and H. Torreblanca, *J. Fusion Energy* **30**, 277–282 (2011).
- <sup>44</sup>R. A. Behbahani and F. M. Aghamir, *Phys. Plasmas* **18**, 103302 (2011).
- <sup>45</sup>S. Lee, S. H. Saw, L. Soto, S. V. Springham, and S. P. Moo, *Plasma Phys. Controlled Fusion* **51**, 075006 (2009).
- <sup>46</sup>S. P. Chow, S. Lee, and B. C. Tan, *J. Plasma Phys.* **8**, 21–31 (1972).
- <sup>47</sup>H. Herold, in *Laser and Plasma Technology*, edited by C. S. Wong *et al.*, Proceedings of Third Tropical College (World Scientific, Singapore, 1990), pp. 21–45.
- <sup>48</sup>B. Freeman, in *Proceedings of the 4th Symposium on Current Trends in International Fusion Research, Washington DC, 2001*, edited by C. D. Orth and E. Panarella (National Research Council of Canada, 2007).
- <sup>49</sup>G. Decker, L. Flemming, H. J. Kaeppler, T. Oppenlander, G. Pross, P. Schilling, H. Schmidt, M. Shakhate, and M. Trunk, *Plasma Phys.* **22**, 245 (1980).
- <sup>50</sup>R. Verma, R. S. Rawat, P. Lee, T. L. Tan, H. Shariff, J. Y. Goh, S. V. Springham, A. Talebitahter, U. Ilyas, and A. Shyam, “Neutron emission characteristics of nx-3 plasma focus device: speed factor as the guiding rule for yield optimization,” *IEEE Trans. Plasma Sci.* (in press).
- <sup>51</sup>A. V. Dubrovsky, V. A. Gribkov, V. N. Pimenov, and M. Scholz, “Comparative characteristics of four small dense plasma focus devices,” *AIP Conf. Proc.* **996**, 103–107 (2008); and Plasma And Fusion Science, 17th IAEA Technical Meeting on Research Using Small Fusion Devices, Lisbon, Portugal 22–24 October 2007.